Water Condensation on Charge Transport Electrical Growth of Nanostructures

Ewa Kowicka, Dmytro Kashyn, Michael A. Keagan, Tadashi Hirano, Pavel S. Paramonov, Ivan Polog, Robert R. Mallik and Sergei F. Lyuksyutov*

Department of Physics, The University of Akron, Akron OH 44325, USA

Abstract: Water condensation under electric field shows a major influence on electrical charge transport and nanostructure formation in polymers.

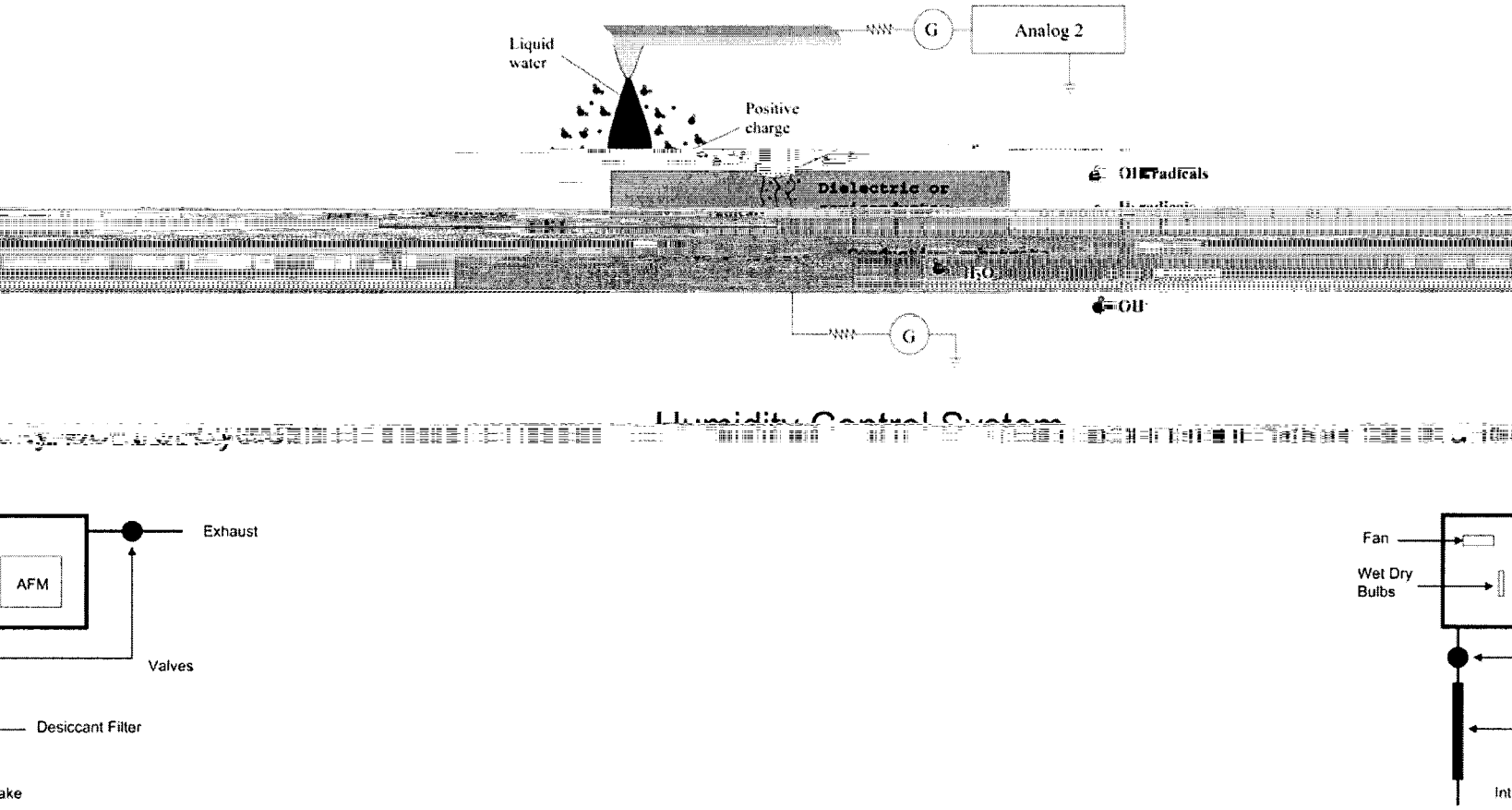

Fig. (1a). Experimental configuration of the optoelectronic system. The system is effective as a nanoscale electrochemical cell. The water monolayer surfaces has been observed to clearly. **(b)** The humidity monitoring, wet/dry bulbs and the humidity was a dynamic gas flow system.

[illegible] series of Wenzel [illegible] active substrate and the ground line current were digitized and recorded on PC.

[illegible] Au-Pd coated silicon wafer substrates. A high purity 99.999% CdS target supplied by Kurt J. Lesker Co. was used as the source material. Sputter [illegible] performed at [illegible] mTorr. [illegible] filtered gas [illegible] desiccant filter [illegible] was used to provide [illegible] Argon [illegible] was used to [illegible] from the gas [illegible] was [illegible] measured [illegible] was monitored continuously [illegible] morphological characterization [illegible] The humidity during the experiment was controlled based on [illegible] the AFM system [illegible] at a pressure [illegible] formed at every [illegible] deposition [illegible] rate [illegible] escape and to avoid [illegible] thickness was [illegible] years [illegible] hours [illegible] was [illegible] are [illegible] [illegible] [illegible]

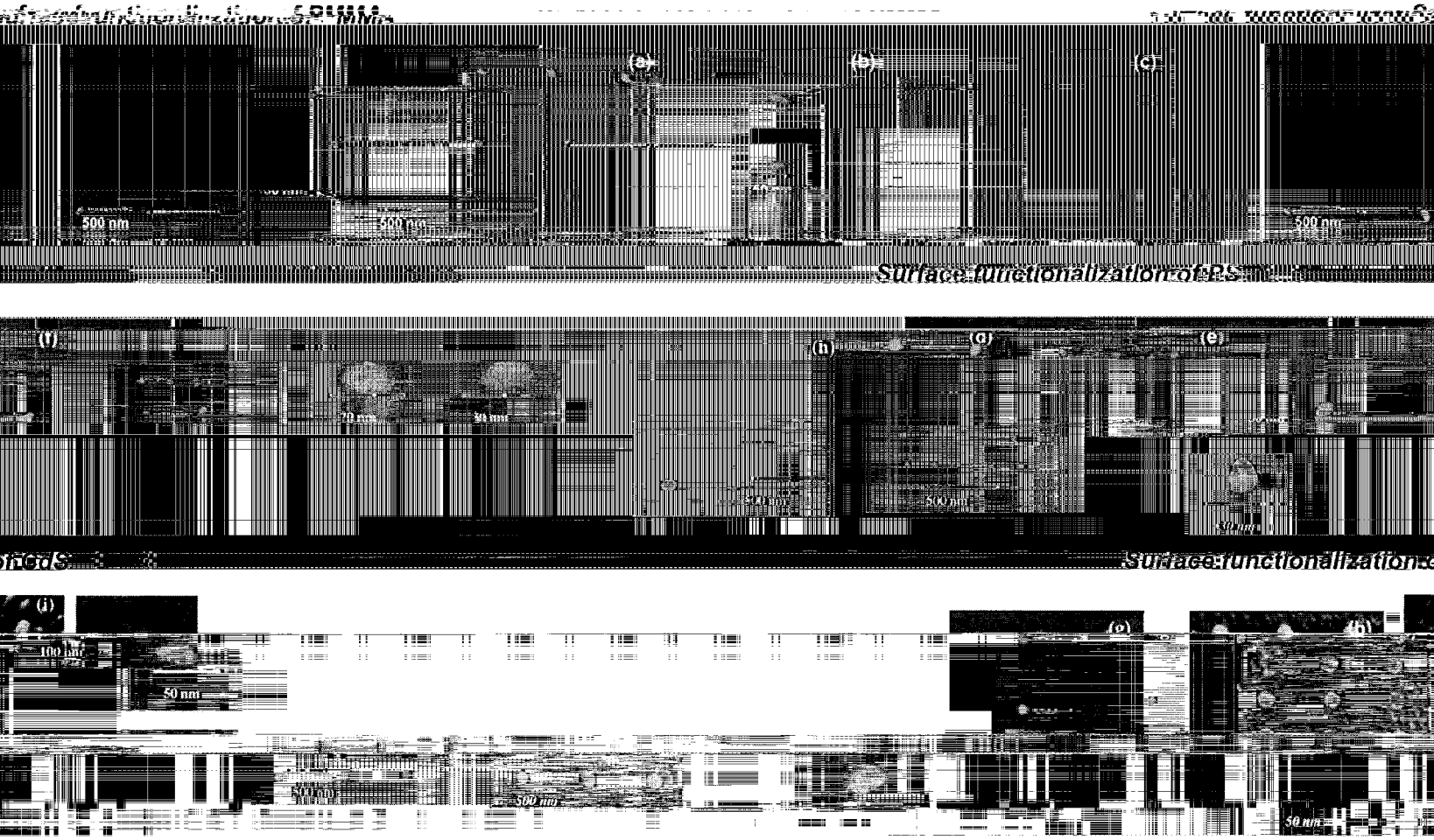

Fig. (2a) through (g). Examples of patterning in a 30 nm thick region of 850k-PMMA film using AFMEN protocol (a) $H_r = 43\%$ [illegible] varies from −6 nA to 1.8 [illegible] producing dots between 50 and 70 nm wide. The height of the dots is between 2 and 4 nm (b) [illegible] varies between 70 and 200 nA [illegible] width of the [illegible]

Fig. (2h) through (l). [illegible] structures [illegible] width of the structures varies between [illegible] and 50 nm [illegible] temperature [illegible] 50%. The [illegible] electric voltage did not exceed −20 V [illegible] **Fig. (2g) through (l).** Nanostructures patterned in 50/100 nm thick PMMA films using same protocol (g) [illegible] 50%. The [illegible] width between [illegible] and [illegible] nm (h) [illegible] 25% An array of dots was patterned [illegible] patterned dots was 40–50 nm, the height of the dots was less than [illegible] nm. [illegible] experiment [illegible] the temperature was maintained around [illegible] °C [illegible]

[illegible] varies between [illegible] and [illegible] nm [illegible] Fig. (2) presents nanographs of the surfaces [illegible] meniscus and [illegible] the effect of [illegible] surface functionalization of the [illegible] the *height* of [illegible] PMMA was observed [illegible] samples [illegible] structures [illegible] and above [illegible] all the samples AFMEN [illegible] was [illegible] tested for the very [illegible] values [illegible] decrease with [illegible] increase [illegible] and 50% Fig. (2h) [illegible] Fig. (2l). One [illegible] nm [illegible] nm [illegible] nm

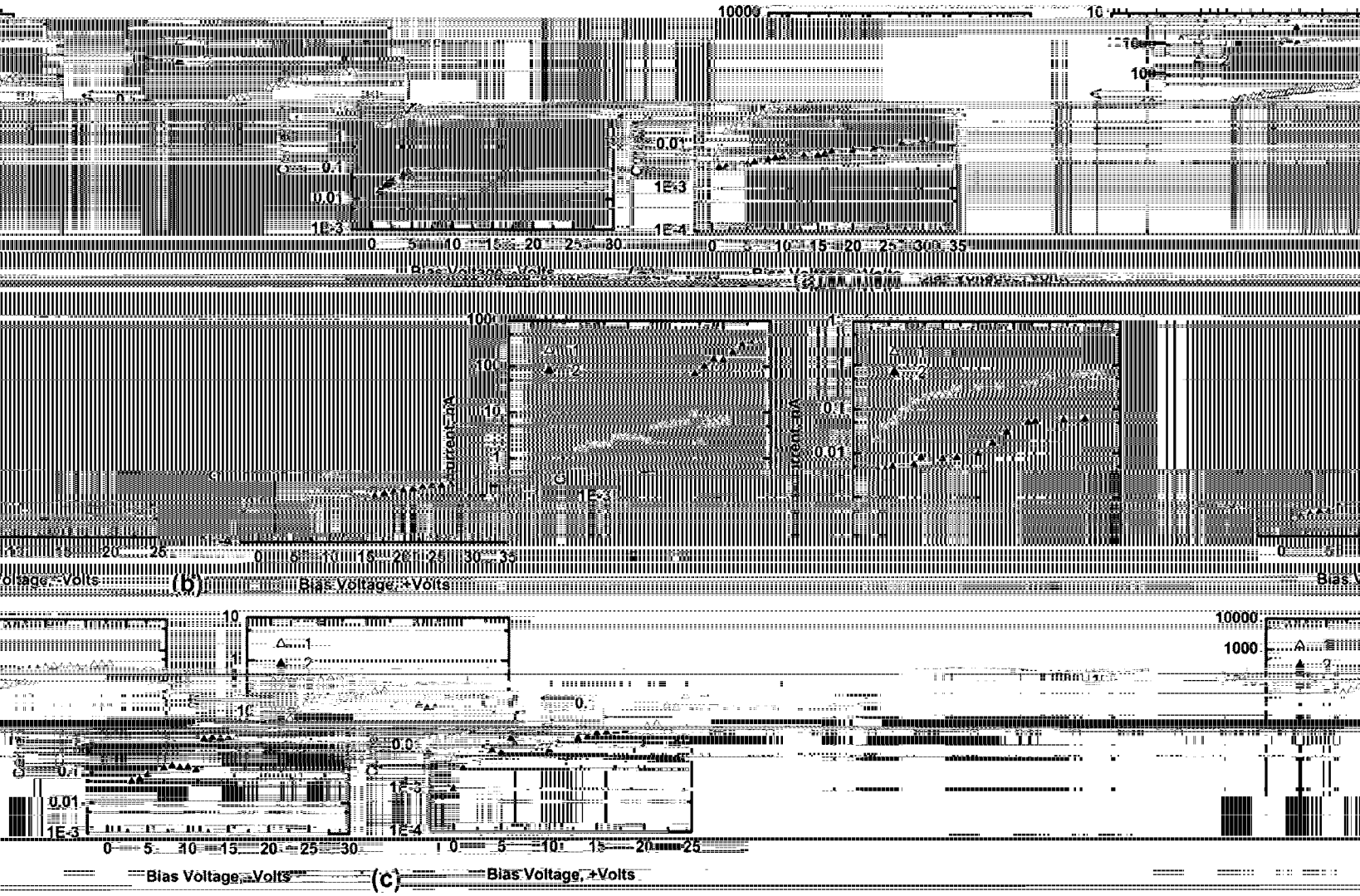

Figure 3. (a) 10-nm PMMA film at H_r = 40%. (b) 30-nm PMMA film at H_r = 20%. (c) 30-nm PMMA film at H_r = 4%.

and 0.1 nA, while the minimum current between 2 and 8 nA ... analyze conductivity processes and charge transport in sub- ... tween 20 nA ... standard samples of 4 nm thick were collected ... measured ... different number levels. Below the above ... breakdown voltage ... PMMA ... substrates. The plots show the input (output) currents ... (3) under negative (a) the input cur- ... PMMA are presented in Fig. 3 at H_r = 40% (Fig. 3a), while the current exhibits changes in steps between ... 20 (b) and 6 ... 12% for negative and positive bias. ... 0.9 and 1.2 and 1.8 and 2.4 and 0.7 nA. Noticeable change of ... defined forward bias when the AFM tip is negative and reverse bias ... the sudden current observed and the evidence of nanostructures ... when it is positive. For the 10-nm PMMA film at H_r = 40% (Fig. ... formed at this level of humidity can be provided. In summary, the ... (c) ... input cur- ... Later ... different ... exceed ... least the order of ... current was observed ... magnitude. The rectangular structures ... an output ... 80 ... for the entire range of bias voltage, although changes ... magnitude ... for the entire range of bias voltage, although changes ... current never exceeded ... 20 to 25 nA ... structures are ... observed ... formed in the polymer surface when the bias current jumps by ... order of magnitude. For positive bias, the input current varies be-

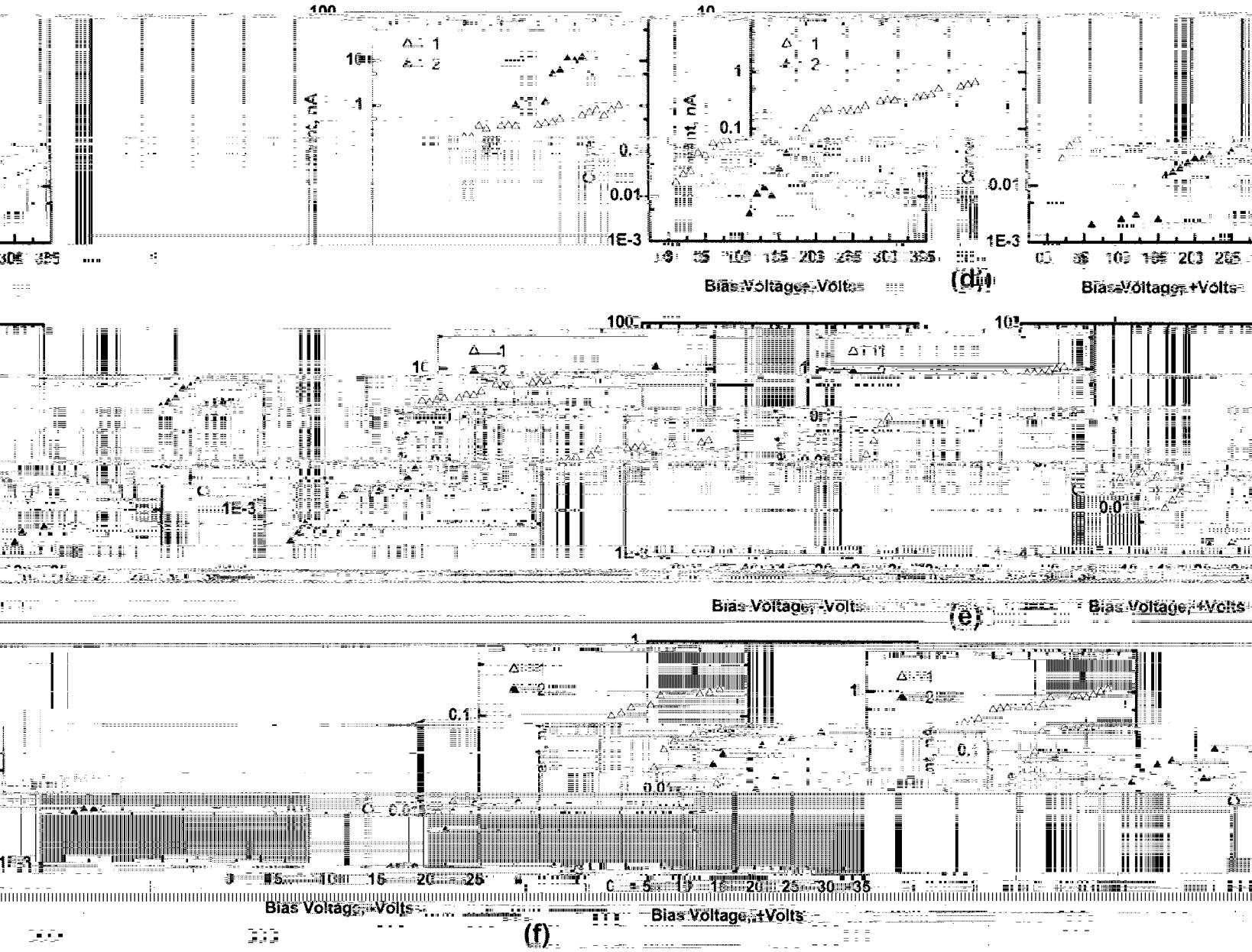

Fig. (3d). through (f). Input (open triangles), and output (closed triangles) currents versus tip bias voltage for a 30-nm PS film **(d)** $H_r = 50\%$, **(e)** $H_r = 26\text{-}30\%$, **(f)** $H_r = 10\text{-}12\%$.

current between 2 and 5 nA. Nanostructures tend to form or [illegible] Results are presented [illegible] of. At $H_r = 10\text{-}12\%$ under negative bias (Fig. 3(f)), [illegible] $H_r = 50\%$ (c) $H_r = 26\text{-}30\%$, (d) $H_r = 0.832\%$ or negative and positive [illegible] current varies between 12 nA (at 250) [illegible] and the output [illegible] tive bias. At $H_r = 50\%$, Fig. (3(d)) and under negative bias the [illegible] current [illegible] between [illegible] and 5 nA (at 2.5 V). [illegible] positive [illegible] input current varies between [illegible] and the output [illegible] [illegible] between [illegible] and [illegible] [illegible] increase [illegible] [illegible] exceed [illegible] [illegible] varying [illegible] [illegible] [illegible]

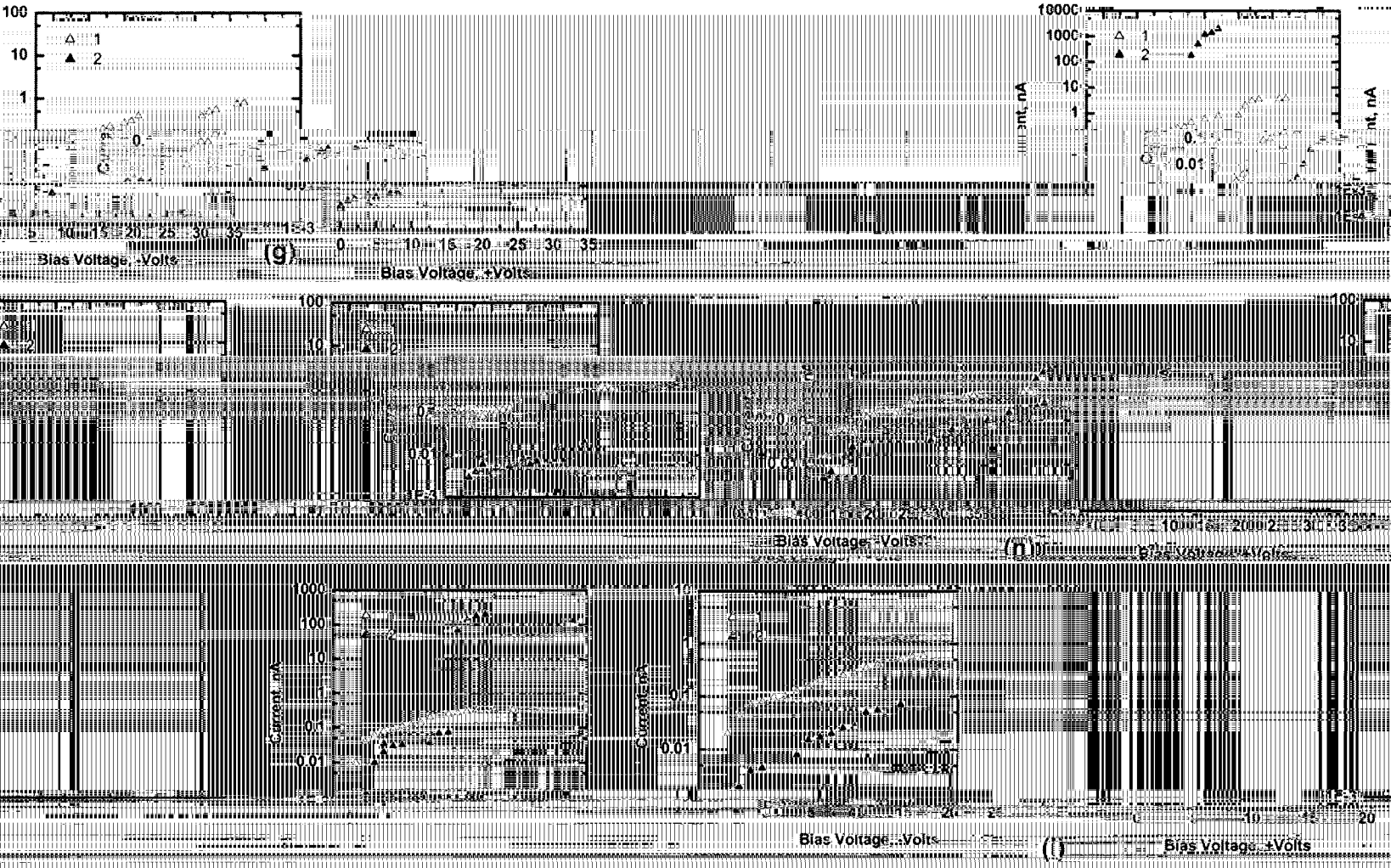

Fig. (3g) through (i): Input (open triangles) and output (closed triangles) currents versus tip bias voltage for a 100 nm CdS film

(g) H_r = 48-50% **(h)** H_r = 20-24 **(i)** H_r = 10-14%

bonding. The thresholds for the pressure and the humidity required ... for (CdS) and polymer (PMMA and PS) films, suggests that the

... surface junction

... further enhances water condensation [20]. When strongly affected ... the surface functionalization with biased AFM tip.

... Electrons in the region between the conductive AFM tip and ... conductive backplane may originate from the three following ...

... ties inside of the polymer film [21]. The fact that ... was found to ...

... factor (A) is not ... major ... electric breakdown as ... served in various polymer films of different chemical structure [19].

... 100 nA) and also through amorphous semiconductor (10-1000 ...

... experimental conditions, this study allows separation of the factor ...

4. SUMMARY

... and the surface functionalization of polymer and semiconductor surfaces, using AFMEN protocol, have been performed for various relative humidity levels. Our results, combined with the previous studies [1, 12] ... that electrons ... by water ionization ...

... junction. Furthermore, the current through the film exceeds the ... current through the tip by an order of magnitude for relative ... 25%. The magnitude of the electric current ...

... humidity levels ...

... meniscus is a likely factor contributing to the large ... ionization is the ... output current.

For the polymer films, the nanostructure formation process is associated with mass transport (displacement) of the macromolecules ... in a strong electric field gradient, while for the semiconductor ... oxidation ...

... different physical and chemical properties, in this case ...

ACKNOWLEDGEMENTS

... AFOSR Grant FA9... E. ... acknowledges the ... Research Associateship ... Faculty Fellowship 2002-2004 awarded by the National ...

REFERENCES

[1] ... M.; Sigalov, G.; Sancaktar, E. *Nat. Mater.* 2003, *2*, 468.
[2] ... S. F.; Vaia, R. A.; Paramonov, P. B.; Juhl, ... *Appl. Phys. Lett.* ... 2003, *82*, 405.
... Sigalov, G. ...
... *Phys. Rev. Lett.* 2004, ... 3836.
... Lyuksyutov, S. F. *Curr. Nanosci.* 2005, ... 245.
[6] ... Sirghi, L. *Appl. Phys. Lett.* 2003, *82*, 3755.
... Garcia, R. *Nanotechnology* ...
[8] ... Gomez-Monivas, S.; Saenz, J. J.; Calleja, M.; Garcia, R. *Phys. Rev. Lett.* 2003, *91*, 056101.
... 14870.
... Paramonov, P. B.; ... Lyuksyutov ...
... Sancaktar, E.; Vaia, R. A.; Juhl, S. *Ultramicroscopy* 2006, ... 909.
[11] ... Bluess ... Staikov, G.; Schultze, ... *Electrochim. Acta* 2001, ... 3335.
[12] ... Lyuksyutov, S. F.; Paramonov, P. B.; Dolog, I.; Ralich, R. M. *Nanotechnology* ...
... Pinkerton, ... Scovell, D. L.; Johnson, A. ...; Xia, B.; Medvedev, V. ...
... *Langmuir* ...
... Gelb, L. D.; Gubbins, K. E.; Radhakrishnan, R.; Sliwinska-Bartkowiak, M. *Rep. Prog. Phys.* 1999, *62*, 1573.
... 2004, *108*, 7814.
[17] ... Weeks, B. L.; Vaughn, M. W.; DeYoreo, J. J. *Langmuir* 2005, *21*, 8096.
... Jiang, ... Schatz, ... *Chem. Phys.* ...
[19] ... Paramonov, P. B.; Lyuksyutov, S. F. *Chem. ...* 2005, ... 984705.
... *State-of-the-Art Compendium*, Wiley: New York, 1988.

Received: September 25, 2007 Revised: November 14, 2007 Accepted: November 20, 2007